

ECOSPHERE

COASTAL AND MARINE ECOLOGY

Growth and feeding in the sponge *Agelas tubulata* from shallow to mesophotic depths on Grand Cayman Island

KEIR J. MACARTNEY, Amelia Clayshulte Abraham, Marc Slattery, and Michael P. Lesser, Marc Slattery, and

¹Department of Molecular, Cellular and Biomedical Sciences, University of New Hampshire, Durham, New Hampshire 03824 USA
²Division of Environmental Toxicology, Department of BioMolecular Science, University of Mississippi, Oxford, Mississippi 38677 USA
³Division of Pharmacognosy, Department of BioMolecular Science, University of Mississippi, Oxford, Mississippi 38677 USA
⁴School of Marine Science and Ocean Engineering, University of New Hampshire, Durham, New Hampshire 03824 USA

Citation: Macartney, K. J., A. Clayshulte Abraham, M. Slattery, and M. P. Lesser. 2021. Growth and feeding in the sponge *Agelas tubulata* from shallow to mesophotic depths on Grand Cayman Island. Ecosphere 12(9):e03764. 10.1002/ecs2.3764

Abstract. On Caribbean coral reefs, sponges are important members of the benthic community and play multiple roles in ecosystem structure and function. They have an important role in benthic-pelagic coupling, consuming particulate organic matter (POM) and dissolved organic matter (DOM) and in turn providing food in the form of sponge biomass or the release of detritus for a variety of coral reef organisms. Throughout the Caribbean, sponges show consistent increases in their abundance and growth rates as depth increases into the mesophotic zone (30-150 m). This has been hypothesized to be driven by bottomup forces, particularly the increased supply of nitrogen-rich POM in mesophotic coral reef ecosystems (MCEs). Here, we tested the hypothesis that the sponge, Agelas tubulata, exhibits increased growth rates on MCEs relative to shallow reefs on Grand Cayman Island and that this is driven by bottom-up forcing. We observed increased growth rates in mesophotic A. tubulata, compared with shallow conspecifics, despite variability in feeding on both POM and DOM. Mesophotic sponges, however, were consistently exposed to greater amounts of POM, which was seasonally variable unlike DOM. Changes in stable isotopic signatures, and higher feeding rates with increasing depth, were consistent with increasing rates of growth in sponges as depth increases. These observations support the hypothesis that mesophotic sponges have higher growth rates due to increased POM availability and consumption over time. The results of this study illustrate the crucial role that bottom-up forcing has in the structuring of sponge communities on both shallow and mesophotic Caribbean coral reefs and the importance of POM as a source of nitrogen in sponge diets.

Key words: coral reefs; dissolved organic matter; mesophotic; particulate organic matter; porifera; sponges; stable isotopes; transplant; trophic ecology.

Received 20 November 2020; revised 6 May 2021; accepted 14 May 2021. Corresponding Editor: Thomas C. Adam. Copyright: © 2021 The Authors. This is an open access article under the terms of the Creative Commons Attribution License, which permits use, distribution and reproduction in any medium, provided the original work is properly cited. † E-mail: kjm1049@wildcats.unh.edu

Introduction

One of the dominant taxa of the benthic fauna on Caribbean coral reefs is sponges, which increase in abundance and biodiversity with increasing depth from shallow to mesophotic depths (10–150 m) (Trussell et al. 2006, Lesser et al. 2009, 2018, 2019, Lesser and Slattery 2013, 2018, Macartney et al. 2021). Sponges have multiple functional roles on coral reefs such as providing food and habitat for many ecologically and economically important coral reef species (Diaz

and Rützler 2001, Bell 2008), reef stabilization (Bell 2008), and in particular, benthic-pelagic coupling (Pile et al. 1997, Lesser 2006, Perea-Blázquez et al. 2012, Lesser and Slattery 2013, Slattery and Lesser 2015). Sponges are also conspicuous on mesophotic coral reefs (MCEs) (Lesser et al. 2009, 2018, Loya et al. 2016, Slattery and Lesser 2019) with communities structured primarily by depth-dependent changes in irradiance and trophic resources (Lesser et al. 2009, 2018, 2019, 2020). Upper MCE (-30-60 m) communities are important refuges for a variety of shallow reef benthic fauna, while lower MCEs (-60-150 m) harbor endemic species that contribute to the unique community structure of the lower MCE (Lesser et al. 2018, 2019). Given the importance of sponges, and the potential role of MCEs as refuges, understanding what factors regulate sponge distributions along the shallow to mesophotic depth gradient will inform predictions on their population dynamics in the future.

Benthic-pelagic coupling by suspension feeders, through the consumption of particulate organic matter (POM) and dissolved organic matter (DOM), supports a large proportion of benthic secondary production (Gili and Coma 1998, de Goeij et al. 2017) and the motile fauna that depend on these resources for food and habitat (Dayton et al. 1974, Diaz and Rützler 2001, Saier 2002, Boudreaux et al. 2006, Bell 2008). The linkage between the planktonic communities and the community structure of benthic suspension feeders has been described for a variety of marine ecosystems including polar, temperate, and tropical benthic communities (Gili and Coma 1998, Cattaneo-Vietti et al. 1999, Menge 2000, Coppari et al. 2016). The role of food availability for suspension feeders is equally important on oligotrophic tropical coral reefs as an important factor influencing sponge abundance and diversity (Lesser 2006, Trussell et al. 2006, Wulff 2017). Several studies have repeatedly observed that bottom-up control is the primary driver of increasing sponge abundances and biomass into the mesophotic zone (Lesser 2006, Trussell et al. 2006, Lesser and Slattery 2013, 2018, Slattery and Lesser 2015, Lesser et al. 2018, 2019, 2020). As depth increases, POM, both heterotrophic picoplankton and prochlorophytes, increases while a concurrent decrease in DOM occurs (Lesser 2006, Trussell et al. 2006,

Lesser et al. 2019, 2020). Since heterotrophic picoplankton and prochlorophytes have lower C: N ratios compared with other cyanobacteria (e.g., *Synechococcus*), it results in increased nitrogen availability with increased depth (Ducklow et al. 1993, Campbell et al. 1994, Lesser 2006).

Increased consumption of picoplankton is associated with increased growth rates in the sponges Callyspongia vaginalis, Agelas conifera (now correctly identified as A. tubulata), and Aplysina fistularis (Lesser 2006). A reciprocal transplant by Trussell et al. (2006) using C. vaginalis between 12 and 25 m showed unequivocally that increased growth rates occur in deeper sponges, and sponges transplanted from shallow to deep habitats where more picoplankton occurred resulted in energy surpluses for deep sponges. Additionally, stable isotope values of δ^{13} C and δ^{15} N became less depleted from shallow to mesophotic depths for both Xestopsongia muta (Morrow et al. 2016) and Agelas tubulata, indicating that these species increasingly rely on POM with increasing depth (Slattery et al. 2011). Related to the increased reliance on POM with increasing depth, Slattery et al. (2016) found that the sponge *Plakortis angulospiculatus* displayed phenotypic variability in chemical defense between shallow and mesophotic specimens; shallow P. angulospiculatus were more chemically defended compared with their mesophotic conspecifics, but mesophotic P. angulospiculatus regenerated tissue faster. This plasticity between chemical defenses and the capacity to repair tissue damage was hypothesized to be the result of increased trophic resources available to mesophotic populations for tissue repair compared with shallow populations.

Sponges also consume DOM, and the microbiome of high microbial abundance sponges (HMA) can consume DOM and translocate byproducts of their metabolism (e.g., dissolved free amino acids) to the host (de Goeij et al. 2008, Freeman and Thacker 2011, Maldonado et al. 2012, Thacker and Freeman 2012, Fiore et al. 2013, 2020, de Goeij et al. 2013, 2017, Shih et al. 2020). However, many of these studies quantified dissolved organic carbon (DOC) but not dissolved organic nitrogen (DON), and while DON is generally an order of magnitude lower in terms of availability compared with DOC (Lesser et al. 2019), it should be quantified to obtain a

complete representation of sponge DOM consumption and reprocessing.

There is a need to integrate feeding measurements with environmental and biochemical data to provide, within a robust experimental framework, evidence to identify and quantify what trophic processes influence sponge distributions. The use of reciprocal transplant experiments provides a quantitative approach to test the null hypothesis that there is no effect of bottom-up processes (i.e., feeding) on the distribution and abundance of sponges, but also whether sponges in the study exhibit phenotypic plasticity in sponge trophic strategy. This design exposes the transplanted sponges to all potential abiotic and biotic factors, including predation, while also allowing for the testing of specific hypotheses on sponge growth along a depth gradient. The sponge used in this study is Agelas tubulata, which is commonly found along the shallow to mesophotic depth gradient in the Cayman Islands. Agelas tubulata is a chemically defended (Pawlik et al. 1995, Richelle-Maurer et al. 2003, Pawlik 2011), HMA sponge that is known to feed on both DOM and POM (Lesser 2006, Slattery and Lesser 2015, de Goeij et al. 2017). Here, we present the results of a reciprocal transplant experiment using A. tubulata to assess changes in growth rates, trophic resource consumption, carbon and nitrogen stable isotopes, and proximate biochemical composition between shallow and mesophotic depths. We hypothesize that the growth rates will be higher in mesophotic control sponges as will the shallow to mesophotic sponge transplants due to the increased availability of particulate organic nitrogen (PON) at those depths and that this will be reflected in their stable isotopic signatures and biochemical composition.

METHODS

Study site

Both the reciprocal transplant and natural growth measurements were conducted at the USS Kittiwake (ASR-13) Anchor Buoy site, Grand Cayman (Lat: 19.362756, Long: –81.402437). This site provides a continuous shallow to mesophotic depth gradient that is characterized by a sloping spur and groove reef structure between 15 and 61 m, at which point reef topography turns into

a vertical wall. Both transplant areas were located on bare coral rock and not on live coral or sand channels.

Light and temperature data

Temperature data were collected along a depth gradient (15, 22, 30, 46, 61, 76, and 91 m) beginning in January 2018 using Hobo Water Temperature Pro V2 loggers attached directly to the substrate using cable ties. Sensors were checked and data downloaded every 6 mo. A drop package was used to obtain profiles of photosynthetically active radiation (PAR: 400-700 nm), for downwelling (E_d) irradiance, as a function of depth using a single channel PAR recorder (RBRsoloPAR; RBR Ltd., Ottawa, Canada) fitted with a calibrated LiCor cosine-corrected, planar, sensor (LI 192SA) combined with a Sea-Bird SBE39 plus temperature and depth profiler. Profiles from the surface to ~100 m depth were taken between 11 AM and 1 PM on partly (25–40%) cloudy days.

Reciprocal transplant and natural growth experiment

To assess changes in growth rates and food consumption, a reciprocal transplant experiment, beginning January 2018, was established between 22 and 61 m. A total of 20 PVC frames (n = 10per depth; Appendix S1: Fig. S1) were affixed to the reef substrate using eye bolts epoxied into the substrate with cable ties placed through the eye bolt and PVC frame. We selected A. tubulata individuals with more than three tubes, tagged them with cow tags (n = 5 at 22 and 61 m), and used them as the source sponges for the transplant study. Five sponge tubes were cut (8–19 cm tall) from these sponges and transplanted from deep (61 m) to shallow (22 m) (DS), and five were transplanted from shallow to deep (SD). Deep to deep (DD) and shallow to shallow (SS) controls (n = 5 each) were also cut and transplanted back to their respective depths of origin as disturbance controls. All samples were identified with a cattle tag on the sponge frame and a plastic growth tag inserted 1 cm below the osculum lip (Appendix S1: Fig. S1). Subsequent measurements from the point of tag insertion to the top of each sponge tube were taken to the nearest 0.1 cm in July 2018, January 2019, and June 2019, and these measurements were used to calculate apical growth rates. Total length and osculum wall thickness (total maximum diameter minus inner diameter) were also measured to the nearest 0.1 cm. Growth rates were reported as apical, total length, and osculum wall thickness in cm/ mo. Unmanipulated A. tubulata along the depth gradient (15–61 m) of the study site (n = 33) were also tagged to provide data on the natural growth rates, assessed as apical growth, across the depth gradient where samples were collected for the transplant experiment. Both transplanted sponges and tagged natural sponges were revisited every 6 mo and growth metrics measured. Additionally, fish bite scars on sponges for each treatment were counted as a relative measure of predation on the experimental sponges. Transplanted sponges were removed from the reef after final measurements at 18 mo. All sponges were kept in a shaded cooler submerged in seawater until they were returned to shore for subsequent analyses. Any samples collected for biochemical and stable isotope analyses were immediately frozen at -20°C and transported frozen to the University of Mississippi or the University of New Hampshire, where they were frozen at -80° C until analysis.

Ambient food availability

To quantify total POM and DOM availability along the shallow to mesophotic depth gradient, replicate water samples (n = 3 per depth) were collected at 0, 15, 22, 30, 46, 61, 76, and 91 m in July 2018 and January 2019. Acid-washed 180mL syringes were filled by divers, taking care not to disturb sediment and detritus, approximately 1 m from the reef substrate. To quantify POM, the samples were returned to the laboratory and 5 mL was aliquoted, fixed at a final concentration of 0.5% electron microscopy grade paraformaldehyde, and frozen at 0°C. Samples were shipped frozen to the University of New Hampshire and stored at -80°C. These samples were subsequently shipped frozen, on dry ice, to the Bigelow Laboratory of Marine Science, J.J. MacIsaac Facility for Aquatic Cytometry where they were stored in liquid nitrogen (-196°C) until analysis. Each sample was analyzed using flow cytometry for total cell abundances, as described and modified by Lomas et al. (2010), using a Becton Dickinson Influx flow cytometer equipped with a 15 mW, 488 nm, air-cooled Argon ion laser. Both Chl a (692 \pm 20 nm) and phycoerythrin (PE, 585 ± 15 nm) bandpass filters were used, and the instrument was calibrated daily with 3.46-µm Rainbow Beads (Spherotech Inc. Lake Forest, Illinois, USA). Each sample was run for 3-5 min (\sim 0.2–0.3 mL total volume analyzed), with logamplified Chl a and PE fluorescence, as well as forward and right-angle scatter signals, recorded, and analyzed using FlowJo 9.8 Software (Becton Dickinson, San Jose, CA). Pico-autotrophs were identified as either Synechococcus, Prochlorococcus, or picoeukaryotes based upon cell size and the presence or absence of phycoerythrin. For pico-autotrophs, the concentration of cells in each population was enumerated and converted to cell abundances by the volume-analyzed method (Sieracki et al. 1993). For heterotrophic bacterial abundance, samples were diluted 1:10 and stained using SYBR™ Green I Nucleic Acid Stain (Thermo Fisher Scientific) at room temperature for 15 min (Marie et al. 2005). Samples were analyzed on a BioRad ZE5 Cell Analyzer using a 488 nm (100 mW) blue excitation laser for a total volume of 100 µl. Files were analyzed from scatter plots based on green (525/35 BP filter) fluorescence and right-angle light scatter (side scatter— SSC) using FlowJo 10 Software (Becton Dickinson, San Jose, CA). Heterotrophic bacterial counts were gated based on cell size and presence of green fluorescence.

All counted cells were converted to their carbon and nitrogen equivalents (sensu Lesser et al. 2019) to provide the concentrations of live particulate organic carbon (POC) and particulate organic nitrogen (PON) available to the sponges. The following conversion values were used: heterotrophic bacteria: 20 fg·C·cell⁻¹ (Ducklow et al. 1993); Prochlorococcus: 53 fg·C·cell⁻¹ (Morel Synechococcus: $470 \text{ fg}\cdot\text{C}\cdot\text{cell}^{-1}$ et al. 1993); (Campbell et al. 1994); heterotrophic bacteria: $3.3 \text{ fg} \cdot \text{N} \cdot \text{cell}^{-1}$ (Fagerbakke et al. 1996); Prochlorococcus: 9.4 fg·N·cell⁻¹; and Synechococcus: 35 fg·N·cell⁻¹ (Bertilsson et al. 2003). For phytoplankton, the carbon and nitrogen contents were computed where C = 0.433 (biovolume, μm^3)^{0.863} and N = 0.883 (biovolume, μm^3)^{0.837} (Verity et al. 1992).

To quantify DOM, 40 mL aliquots were collected from the same water samples used for flow cytometry analyses. These samples were filtered through a 0.2-µm GF/F filter and

immediately frozen at 0°C and transported frozen to the University of New Hampshire. The filtered seawater samples were analyzed at the UNH Water Quality Analysis Laboratory. Dissolved organic carbon (DOC, μ mol·C·L⁻¹) and dissolved organic nitrogen (DON, μmol·N·L⁻¹) were quantified using high-temperature catalytic oxidation and high-temperature oxidation with chemiluminescent detection, respectively. Dissolved inorganic nitrogen (DIN) as NO_x (i.e., $NO_3^- + NO_2^-$), ammonium (NH₄), phosphate (PO₄), and silicon dioxide (SiO₂) were analyzed using a SmartChem 200 automated colorimetric chemistry analyzer (Wesco, Brookfield, Connecticut, USA) or a Seal AQ2 (Seal Analytical, Mequon, WI, USA) discrete colorimetric analyzer. Standard EPA protocols for each compound (NO_x: #353.2, NH₄: #350.1, PO₄: #365, SiO_2 : #370.1) were used.

Sponge feeding measurements

To assess sponge feeding, paired ambient and ex-current water samples were collected from each transplant and control sponge in July 2018 and January 2019. Feeding samples from tagged, naturally occurring, sponges were collected in January 2019. Ambient water samples were collected approximately 10 cm from the base of a sponge tube, and ex-current samples were collected in acid-washed 180-mL syringes with surgical tubing inserted approximately halfway down the osculum of the sponge (Lesser 2006). POM and DOM were quantified as described above. After feeding samples were collected, sponge pumping rates were assessed using fluorescein dye injected at the base of the tube; the time of appearance of the dye at the osculum was recorded (s⁻¹). Morphometrics on each sponge was collected to calculate the volume of a cylinder (= plug volume) using total length of the tube and osculum width to the nearest 0.1 cm. In order to calculate a Q value (volume flux, mL s⁻¹), the cross-sectional area (cm²) of the sponge osculum was calculated and multiplied by the dye front speed (cm s⁻¹). This was calculated by dividing the total tube length of the sponge by the dye speed (Trussell et al. 2006), and the method assumes plug flow through the sponge tube, and a visual assessment of the dye fronts produced during measurements confirms plug flow in the sampled sponges.

To calculate sponge feeding on POM, filtration efficiency was calculated for each sponge by dividing the concentrations of total cells in the sponge ex-current water samples by the concentration of total cells in the ambient water samples taken adjacent to the sponge and multiplied by 100. Total cells consumed for each class (i.e., prochlorophytes, Synecochoccus, eukaryotic phytoplankton, and heterotrophic bacteria) of cells were computed by multiplying the ambient concentration of cells (cells/mL) by the filtration efficiency of cells and the Q value (mL s⁻¹) for each sponge. All filtered cells were then converted to carbon or nitrogen equivalents as described above. Rates of carbon or nitrogen uptake (µg s⁻¹) were calculated by multiplying cells filtered by the relevant group's carbon or nitrogen equivalencies per cell, and then, they were converted to molar equivalents (µmol s⁻¹). Similarly, to calculate sponge feeding on DOM, filtration efficiency was calculated for each sponge by dividing the concentrations of total DON or DOC in the sponge ex-current water samples by the concentration of total DON or DOC in the ambient water samples taken adjacent to the sponge and multiplied by 100. Instantaneous total DON or DOC consumed (s⁻¹) was computed by multiplying the ambient concentration of DON or DOC (μmol L⁻¹) by the filtration efficiency and the individual sponge Q value (L s⁻¹). The dry mass of each sponge (g) was calculated using a tissue density of 0.14 g mL⁻¹ for A. tubulata (Weisz et al. 2008).

Stable isotope analyses

Subsamples of *A. tubulata* tissue were collected from experimental sponges in June 2019 at the end of the experiment using a sterile razor. Tissue samples were dried at 55°C for 24 h and powdered using a mortar and pestle. Samples of powdered tissue were sent to the Marine Biological Laboratory (Woods Hole, MA) for bulk analysis of C and N, as well as the natural abundance of the stable isotopes δ^{15} N and δ^{13} C. Prior to analysis, samples were acidified using 1 M HCL, and our analysis of acidification on δ^{15} N tissue values (sensu Vafeiadou et al. 2013) revealed no significant effects on our samples, as previously reported (Jaschinski et al. 2008, Kolasinski et al. 2008). Samples were analyzed using a Europa ANCA-SL elemental analyzer-gas chromatograph

attached to a continuous-flow Europa 20–20 gas source stable isotope ratio mass spectrometer. The carbon isotope results are reported relative to Vienna Pee Dee Belemnite, and nitrogen isotope results are reported relative to atmospheric air, and both are expressed using the delta (δ) notation in units per mil (%). The analytical precision of the instrument was \pm 0.1%, and the mean precision of sample replicates for δ^{13} C was \pm 0.4%0 and δ^{15} N was \pm 0.2%0.

Proximate biochemical composition

The samples collected in June 2019 were freeze-dried and pulverized, and dry sample mass was recorded. Carbohydrates were extracted via incubation of 10 mg freeze-dried tissue in 5 mL 5% trichloroacetic acid (TCA) for 4 h. Concentration of carbohydrates was determined using the phenol-sulfuric acid method in microplate format described in Masuko et al. (2005). Briefly, 50 µl of TCA-digested sample solution or glucose standard, 150 µl of sulfuric acid, and 30 µl of 5% phenol were pipetted in triplicate on a 96-well plate and incubated for 10-15 min at 90°C. Absorbance at 490 nm was then measured using a BioTek Synergy HT Multi-Detection Microplate Reader. A standard curve was derived from glucose standards and used to calculate the concentration of carbohydrates in samples. Soluble protein was extracted via incubation of 10 mg of freeze-dried tissue in 5 mL of 1 M sodium hydroxide (NaOH) for 24 h. Soluble protein concentration was then analyzed using the Bradford Method (Bradford 1976). Briefly, 40 μl of NaOH-digested sample or BioRad Bovine Serum Albumin (BSA) standard was mixed with 2 mL of BioRad Quick Start™ Bradford reagent. Absorbance at 600 nm was measured using an 8.5-mm Eppendorf BioPhotometer. A standard curve was derived from BSA standards and used to calculate the concentration of protein in samples. Lipids were extracted using a modified version of the protocol described by Freeman et al. (1952). A 50 mg sample of freeze-dried tissue was sonicated for 15 min in a 2:1 chloroform to methanol solution and then filtered into a 50 mL conical tube containing -20 mL of distilled water. The bottom organic layer was then pipetted into a pre-weighed scintillation vial. This process was repeated twice per sample. The methanol-chloroform solution was

then evaporated off over a period of 12 h via vacuum centrifugation, and the final mass of the dry lipid fraction was recorded. Inorganic tissue constituents (i.e., ash) were measured using methods described by McClintock et al. (1991). A 100 mg sample of freeze-dried sponge tissue was placed in a pre-weighed aluminum foil weigh boat that was baked at 500°C in a muffle furnace for 5 h to obtain the ash content of each sample. All concentrations of proximate biochemical composition were normalized to ash-free dry weight (AFDW). Refractory material was calculated by subtraction of all the measured components from the total sponge tissue mass and is known as AFDW. This fraction is technically comprised of additional biochemical compounds, such as nucleic acids their contributions to mass are generally considered negligible, so the refractory material is assumed to represent insoluble protein (Lawrence 1973).

Statistical analyses

All statistical analyses were completed in either JMP (v. 14) or R (v. 3.6.2). Mean monthly and yearly temperatures were tested using a oneway ANOVA with depth as the fixed factor, and the effect of depth on PAR was assessed using a non-linear regression. Sponge growth rates in the transplant experiment were assessed using a one-way ANOVA with treatment (i.e., transplant and transplant controls) as the fixed factor, and the growth rate of unmanipulated sponges was quantified using linear regression. To assess differences between depths and years in the concentration of available POM and DOM, an analysis of covariance (ANCOVA) was run using depth as a fixed factor and year as the covariate. In order to assess differences in sponge consumption of POM and DOM between treatments, an analysis of covariance (ANCOVA) was run with treatment as the primary factor and sponge dry mass (calculated as described in the sponge feeding section) as the covariate; this removed the potential allometric effects of sponge size on sponge pumping and food intake. Because all analyses showed that the slopes were nonhomogeneous, where homogeneity of slopes is a requirement for an ANCOVA, individual regression slopes from each treatment were used to weight individual sponge pumping or feeding rates to a sponge of standard dry mass (Packard

6

and Boardman 1988, Lesser and Kruse 2004). The weighted feeding rates were then analyzed using an ANOVA with experimental treatment as the fixed factor.

The statistical analyses for treatment effects on SIA and proximate biochemical compositions were carried out utilizing an ANOVA. Any variables not meeting the assumptions of normality were log-transformed before analysis. Any significant global effects of treatment detected by ANOVA were followed up with post hoc multiple comparison tests using Tukey's HSD tests.

RESULTS

Light and temperature

There was a significant effect of depth on mean daily temperature in July 2018 (ANOVA: $F_{6,90} = 87.51$, P = <0.001) but not in January 2019 (ANOVA: $F_{6,170} = 1.283$, P = 0.267) (Fig. 1, Appendix S1: Table S1). In July 2018, the mean monthly temperature was 29.25°C (\pm 0.45 SD) at 22 m and 28.09°C (\pm 0.19 SD) at 61 m. In January

2019, mean monthly temperature was 27.38°C (\pm 0.18 SD) at 22 m and 27.42°C (\pm 0.19 SD) at 61 m. The attenuation of E_d with depth was typical for tropical case I or II waters (Lesser et al. 2009) (Appendix S1: Fig. S3). At 22 m, E_d was -198 µmol quanta·m⁻²·s⁻¹, and at 61 m, E_d was -96 µmol quanta·m⁻²·s⁻¹.

Transplant experiment and natural growth of sponges

There was a significant effect of treatment on apical growth rates (ANOVA: $F_{3,16} = 8.51$, P = 0.001). Sponges from the DD and SD treatments had a significantly higher mean growth rate (DD = 0.12 ± 0.01 [SE] cm mo⁻¹, SD = 0.11 ± 0.02 [SE] cm mo⁻¹) than DS transplants (DS = 0.02 ± 0.01 [SE] cm mo⁻¹) (Tukey's HSD = <0.05) (Fig. 2A), which had the lowest growth rates of all treatments. Samples from the SS treatment showed an intermediate mean growth rate (SS = 0.07 ± 0.04 [SE] cm mo⁻¹) that was not significantly different from any other treatment group (Fig. 2A). There was a significant effect of

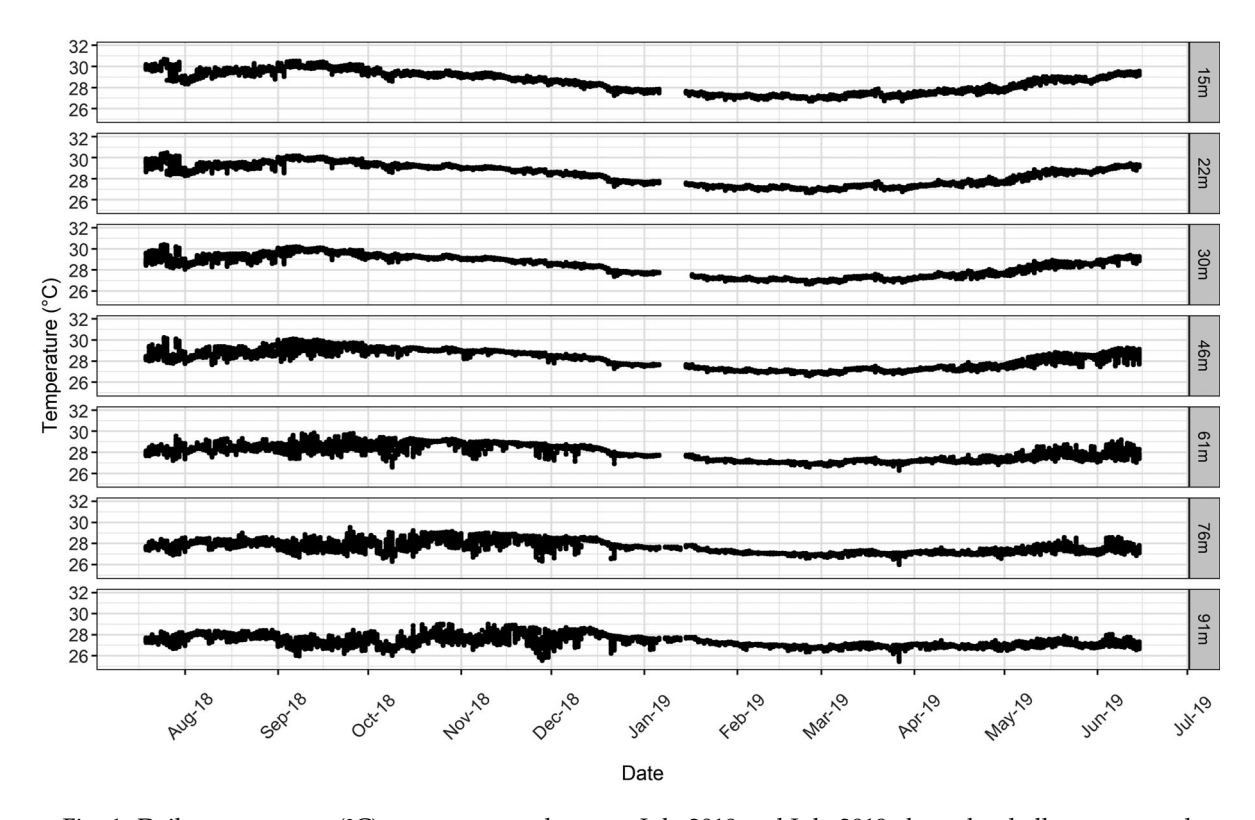


Fig. 1. Daily temperature (°C) measurements between July 2018 and July 2019 along the shallow to mesophotic depth gradient at the experimental site.

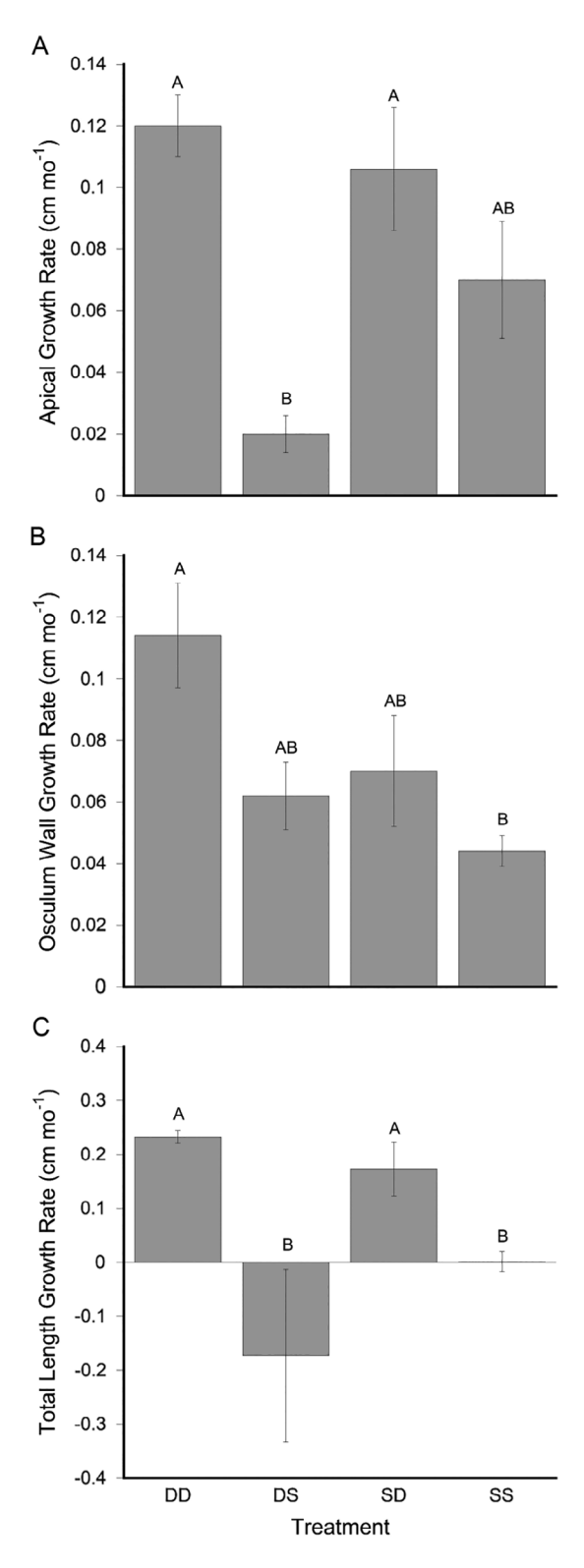


Fig. 2. Experimental transplant effects between

treatment on osculum wall width (ANOVA: $F_{3.16} = 4.27$, P = 0.021). Sponges from the DD treatment had significantly greater osculum wall width growth rates (DD = 0.11 ± 0.02 [SE] cm mo⁻¹) than the sponges from SS treatment $(SS = 0.04 \pm 0.005 \text{ [SE]} \text{ cm mo}^{-1})$ (Tukey's HSD = <0.05) (Fig. 2B). Treatment also had a significant effect on the total length of sponges (ANOVA: $F_{3,16} = 4.25$, P = 0.025) with DD sponges (DD = 0.23 ± 0.012 [SE] cm mo⁻¹) displaying significantly higher growth rates compared with DS transplants (DS = -0.17 ± 0.16 [SE] cm mo⁻¹) (Tukey's HSD = <0.05) (Fig. 2C). There was also a significant effect of depth on the apical growth rates of naturally occurring, unmanipulated, sponges (t(25) = 6.31, P = 0.0188), as well as growth rates based on total length (t (31) = 12.62, P = 0.0012) using linear regression, with deeper sponges displaying the highest growth rates (Fig. 3A, B). There was no significant effect of depth on osculum wall width growth rates (t(25) = 0.23, P = 0.6334) (Fig. 3C).

Ambient levels of POM and DOM

For POC (μ mol·C·L⁻¹), the regression lines were homogeneous (ANCOVA: depth x year interaction, $F_{1,15} = 0.0001$, P = 0.992) while both depth (ANCOVA: $F_{1,15} = 9.67$, P = 0.009) and year (ANCOVA: $F_{1,15} = 88.03$, P < 0.0001) showed a significant effect on POC concentrations which increased with increasing depth. As depth increased into the mesophotic zone, the available POC during the July 2018 sampling period was significantly greater compared with January 2019 (Fig. 4A). The regression lines for PON $(\mu \text{mol}\cdot \text{N}\cdot \text{L}^{-1})$ were not homogeneous (ANCOVA: depth \times year interaction, $F_{1,15} = 6.76$, P = 0.023). While PON increased significantly with depth (ANCOVA: $F_{1,15} = 37.42$, P < 0.0001), the effect of year was assessed using a separate Bonferronicorrected ANOVA. Using the more stringent P = 0.025 value, a significant effect (ANOVA: $F_{1.15} = 88.03$, P = 0.006) for year was observed, with PON significantly greater in July 2018 com-

(Fig. 2. Continued)

treatments on mean (\pm SE) (A) apical growth rate, (B) osculum wall thickness growth rate, and (C) total length growth rate. Levels not connected by the same letter are significantly different (Tukey's HSD < 0.05).

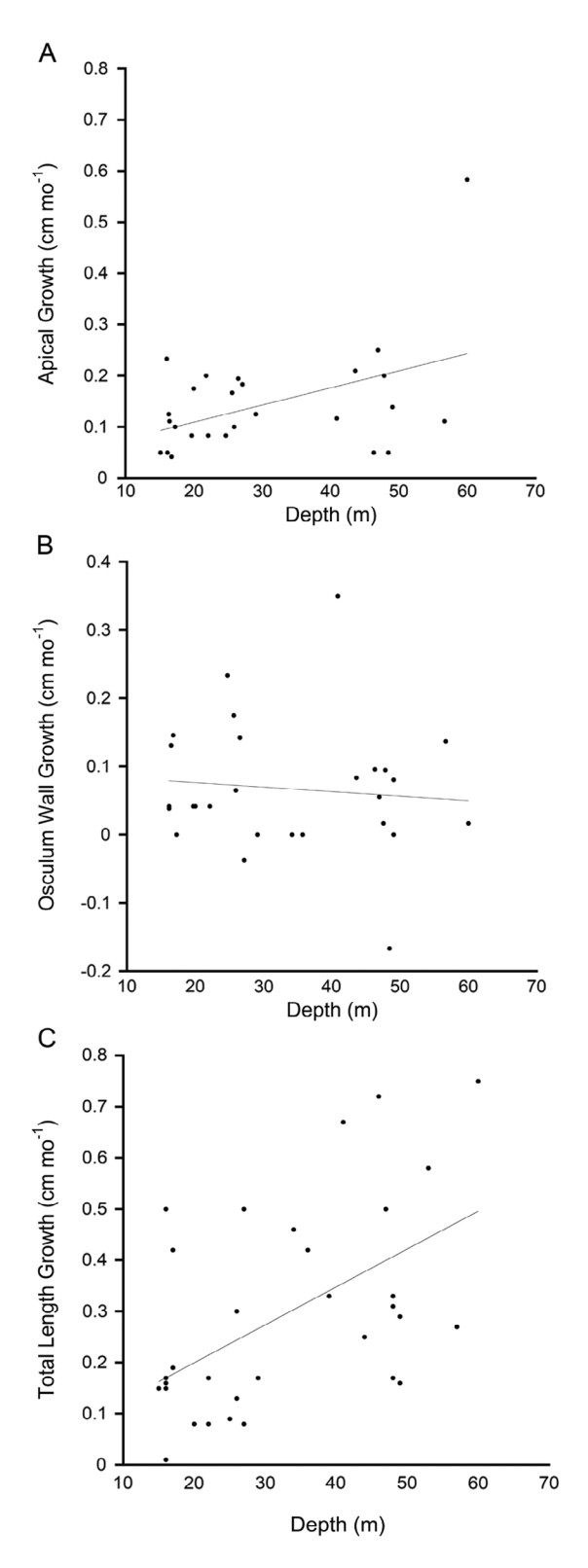


Fig. 3. Effects of depth (m) on (A) apical growth rate

pared with January 2019 (Fig. 4B). For DOC (µmol·C·L⁻¹), the regression lines were homogeneous (ANCOVA: depth × year interaction, $F_{1,15} = 0.186$, P = 0.674), while depth (Fig. 4C) had a significant effect (ANCOVA: $F_{1,15} = 29.17$, P = 0.0002) and year was not significant (ANCOVA: $F_{1,15} = 1.05$, P = 0.326). For DON (µmol·N·L⁻¹), the regression lines were homogeneous (ANCOVA: depth × year interaction, $F_{1,15} = 2.914$, P = 0.114), while depth (Fig. 4D) showed a significant effect (ANCOVA: $F_{1,15} = 55.81$, P < 0.0001), and the effect of year on DON concentration was not significant (ANCOVA: $F_{1,15} = 0.30$, P = 0.594).

The regression lines for NO_x (µmol L⁻¹) were not homogeneous (ANCOVA: depth x year $F_{3.47} = 6.36$, interaction, P < 0.0001). increased significantly with depth (ANCOVA: $F_{3.47} = 234.36$, P < 0.0001), and the effect of year was assessed using a separate Bonferronicorrected ANOVA. Using the more stringent P = 0.025 value, a significant effect (Bonferronicorrected ANOVA: $F_{1,47} = 16.39$, P = 0.0002) for year was observed. NO_x was significantly greater in January 2019 compared with July 2018 (Appendix S1: Fig. S4). The regression lines for PO₄ (Appendix S1: Fig. S4) were not homogenous (ANCOVA: depth x year interaction, $F_{3,47} = 4.37$, P = 0.0349), and there was no significant effect of depth (ANCOVA: $F_{1.47} = 0.8423$, P = 0.363) or year (Bonferroni-corrected ANCOVA: $F_{1,47} = 0.04$, P = 0.984). The regression lines for SiO₂ (Appendix S1: Fig. S4) were not homogenous (ANCOVA: depth × year interaction, $F_{3,44} = 0.816$, P = 0.627), and no significant effect of depth (ANCOVA: $F_{1.47} = 0.625$, P = 0.28) or year (Bonferroni-corrected ANOVA: $F_{1,47} = 0.62$, P = 0.434) was observed.

Sponge consumption of POM and DOM, and nutrient fluxes

Because *Q* values calculated for the transplant and control sponges on the transplant racks were consistently much lower than for unmanipulated

(Fig. 3. Continued)

 $(y = 0.042267 + 0.003351x, R^2 = 0.20188, P = 0.0188)$, (B) osculum wall thickness growth rate $(y = 0.08968 + 0.006567x, R^2 = 0.0092, P = 0.6334)$, and (C) total length growth rate $(y = 0.051545 + 0.007405x, R^2 = 0.28094, P = 0.0012)$ in the sponge *Agelas tubulata*.

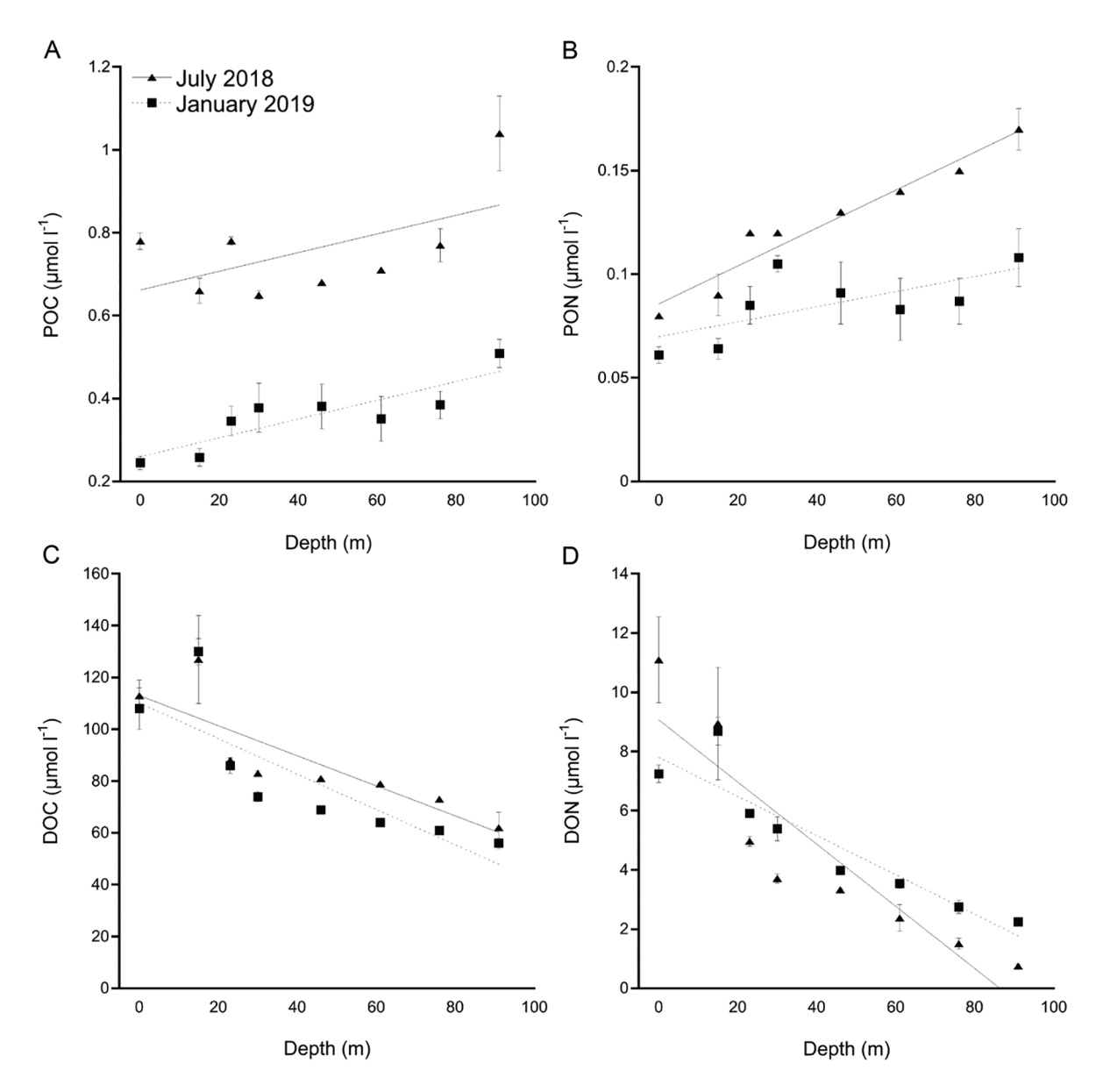


Fig. 4. Effects of depth on mean (\pm SE) ambient concentrations of (A) particulate organic carbon (POC) (July 2018: y=0.6625+0.002261x, $R^2=0.318$, P<0.0001; January 2019: y=0.25962+0.00225x, $R^2=0.752$, P<0.0001), (B) particulate organic nitrogen (PON) (July 2018: y=0.0858+0.000916x, $R^2=0.938$, P<0.0001; January 2019: y=0.0699+0.000362x, $R^2=0.458$, P<0.0001), (C) dissolved organic carbon (DOC) (July 2018: y=113.1-0.5813x, $R^2=0.731$, P<0.0001; January 2019: y=110.28-0.6848x, $R^2=0.698$, P<0.0001), and (D) dissolved organic nitrogen (DON) (July 2018: y=9.0764-0.1049x, $R^2=0.821$, P<0.0001; January 2019: y=7.8-0.06625x, $R^2=0.857$, P<0.0001).

sponges (Appendix S1: Fig. S2), we used the mean Q value (mL s⁻¹) measured for the source sponge populations at their respective depths of 22 and 61 m for all calculations. The transplanted

sponges did not fully attach to the PVC rack which resulted in the loss of head pressure, and the lower volume fluxes in the experimental sponges were an artifact of transplantation. All feeding rates were calculated from the actual filtering efficiencies of experimental sponges using the respective *Q* values from naturally occurring sponges at the experimental depths. All feeding rates are estimated rates.

For the feeding studies in both July 2018 and January 2019, there were violations in the assumptions (i.e., homogeneity of slopes) of ANCOVA for all dependent variables. As a result, all analyses were conducted using a weighted ANCOVA approach as described above. There were significant treatment effects for POC uptake $(\mu \text{mol} \cdot \text{C} \cdot \text{s}^{-1})$ in July 2018 (ANOVA: $F_{3,17} = 6.34$, P = 0.0061) with the SD treatment having the highest rate among treatments. Post hoc multiple comparisons showed that the DD and SS treatments were intermediates and the DS treatment had the lowest uptake of POC (Tukey's HSD: P < 0.05) (Table 1). For PON uptake $(\mu \text{mol} \cdot \text{N} \cdot \text{s}^{-1})$, there were significant treatment effects (ANOVA: $F_{3,17} = 4.99$, P = 0.014) with the SD treatment having the highest rate among treatments. Post hoc multiple comparisons showed that the DD and SS treatments were intermediates and the DS treatment had the lowest uptake of PON (Tukey's HSD: P < 0.05) (Table 1). For DOC (μ mol·C·s⁻¹), there were significant treatment effects (ANOVA: $F_{3.17} = 14.01$, P = 0.0002) with the SD and DD treatment having the highest rate among treatments while the DS and SS treatments had lower mean uptake (Tukey's HSD: P < 0.05) (Table 1). Similarly, for DON uptake (μ mol·N·s⁻¹) there were significant treatment effects (ANOVA: $F_{3.17} = 5.07,$

P=0.0139) with the DD treatment having the highest rate among treatments. Post hoc multiple comparisons showed that the only significant pair-wise difference was between the SS and DD treatments (Tukey's HSD: P<0.05) (Table 1). For January 2019, only the uptake of DOC was significantly different between treatments (ANOVA: $F_{3,17}=3.64$, P=0.0393), with the DD treatment showing significantly higher DOC uptake compared with all other treatments (Tukey's HSD: P<0.05) (Table 1).

There were no significant effects of treatment for fluxes of NO_x , NH_4 , PO_4 , or SiO_2 (Appendix S1: Table S2). These were then binned based on their final depth of occurrence for experimental sponges (22 m = SS and DS treatments and 61 m = DD and SD treatments). There were no significant differences between depths in July 2018 (Table 2) but in January 2019, sponges at 61 m produced significantly more DIN (ANOVA: $F_{3,32} = 27.91$, P < 0.0001) and NH_4 (ANOVA: $F_{3,32} = 8.99$, P = 0.008) (Table 2). There was a significant effect of year for DIN flux (ANOVA: $F_{3,32} = 3.56$, P = 0.0385) with sponges in January 2019 having higher rates of DIN production compared with July 2018.

Stable isotope analyses

For *Agelas tubulata*, there were no significant differences for δ^{13} C (ANOVA: $F_{3,17} = 2.31$, P = 0.121), δ^{15} N (ANOVA: $F_{3,17} = 2.72$, P = 0.084), or molar C:N ratios (ANOVA: $F_{3,17} = 2.32$, P = 0.119) between treatments (Table 1). Samples were then binned by final collection depth (22)

Table 1. Mean (\pm SE) feeding rates from experimental sponges and natural sponges between treatments.

Date	Treatment	DOC (µmol/s)	Tukey's HSD	DON (µmol/s)	Tukey's HSD	POC (μmol/s)	Tukey's HSD	PON (μmol/s)	Tukey's HSD
July 2018	DD	34.45 ± 1.6	A	1.36 ± 0.16	A	0.237 ± 0.057	AB	0.044 ± 0.011	AB
	SD	26.14 ± 4.0	A	0.92 ± 0.14	AB	0.324 ± 0.068	A	0.06 ± 0.013	A
	DS	11.64 ± 1.58	В	0.92 ± 0.3	AB	0.051 ± 0.015	В	0.007 ± 0.003	В
	SS	9.84 ± 2.87	В	0.72 ± 0.08	В	0.158 ± 0.037	AB	0.027 ± 0.011	AB
January 2019	DD	17.89 ± 4.67	A	3.62 ± 0.28	A	0.105 ± 0.025	A	0.019 ± 0.004	A
	SD	8.07 ± 0.74	В	1.73 ± 0.37	A	0.2 ± 0.0496	A	0.036 ± 0.009	A
	DS	2.23 ± 1.19	В	0.31 ± 0.06	A	0.095 ± 0.041	A	0.016 ± 0.007	A
	SS	9.41 ± 3.66	В	3.23 ± 1.54	A	0.086 ± 0.003	A	0.016 ± 0.001	A
January 2019	Unmanipulated 22 m	3.79 ± 1.44	A	0.43 ± 0.07	A	0.171 ± 0.022	A	0.029 ± 0.004	A
	Unmanipulated 61 m	12.63 ± 2.83	A	0.86 ± 0.28	A	0.2 ± 0.041	A	0.036 ± 0.008	A

Note: Levels not connected by a common letter are significantly different (Tukey's HSD, P < 0.05).

		1 0	1 1		
Date	Depth (m)	NO _x flux (μmol/s)	NH ₄ flux (μmol/s)	PO ₄ flux (μmol/s)	SiO ₂ flux (μmol/s)
July 2018	22	-0.006 ± 0.008	0.067 ± 0.064	-0.0005 ± 0.006	0.024 ± 0.026
•	61	-0.017 ± 0.059	0.353 ± 0.267	0.0005 ± 0.002	-1.119 ± 1.812
January 2019	22	0.012 ± 0.007	0.001 ± 0.067	-0.0012 ± 0.001	-0.007 ± 0.028
•	61	0.131 ± 0.021	0.361 ± 0.098	-0.0009 ± 0.003	0.592 ± 0.575

Table 2. Mean (\pm SE) nutrient fluxes of nitrate and nitrite (NO_x), ammonium (NH₄), phosphate (PO₄), and silica dioxide (SiO₂) in experimental sponges between transplant depths.

and 61 m), and significant differences between the two depths for δ^{13} C (ANOVA: $F_{3,17}=5.47$, P=0.0326), δ^{15} N (ANOVA: $F_{3,17}=7.36$, P=0.0153), and molar C:N ratios (ANOVA: $F_{3,17}=6.61$, P=0.02) were observed. There was enrichment in both δ^{13} C and δ^{15} N and a lower molar C:N ratio in the 61 m samples (Fig. 5, Appendix S1: Table S3).

Proximate biochemical composition

There were no significant treatment effects observed for the concentration of carbohydrates (ANOVA: $F_{3,16} = 0.24$, P = 0.867), lipids (ANOVA: $F_{3,16} = 1.12$, P = 0.378), soluble proteins (ANOVA: $F_{3,16} = 0.36$, P = 0.787), insoluble proteins (ANOVA: $F_{3,16} = 0.23$, P = 0.871) normalized to AFDW, or total energetic content in J mg⁻¹ AFDW (ANOVA: $F_{3,16} = 0.78$, P = 0.535) (Appendix S1: Table S4).

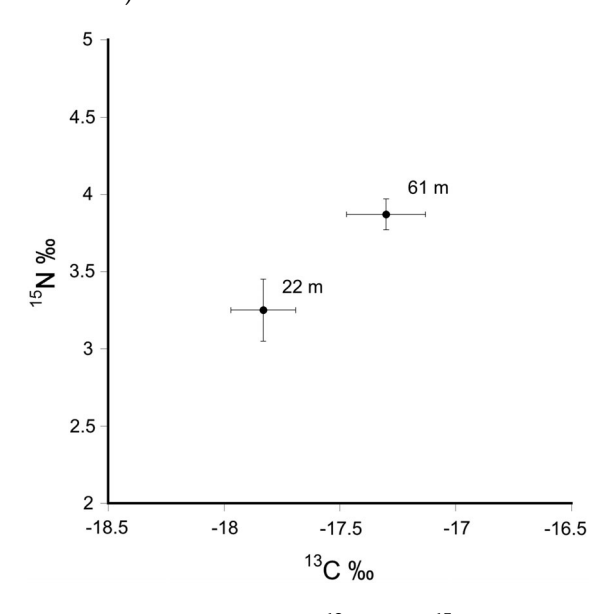


Fig. 5. Bivariate plot of $\delta^{13}C$ and $\delta^{15}N$ bulk tissue stable isotopes binned by depth (mean \pm SE) from the *Agelas tubulata* transplant experiment.

Bite scars on experimental samples

There were no fish bite scars observed on any *A. tubulata,* either natural or experimental samples, during the duration of the experiment.

Discussion

Manipulated and unmanipulated sponge growth rates increase as depth increases

The biodiversity and abundances of sponges on Caribbean mesophotic coral reefs (30–150 m) show a repeatable pattern of increased abundances and biodiversity (Lesser 2006, Trussell et al. 2006, Lesser and Slattery 2013, 2018, Slattery and Lesser 2015, Lesser et al. 2018, 2019). Populations of *A. tubulata* on the Cayman Islands also show a significant increase in percent cover with increasing depth (Macartney et al. 2021). The results of this reciprocal transplant study show that for the emergent HMA sponge, A. tubulata, populations from mesophotic depths have a higher growth rate relative to conspecifics located at depths <30 m. Both the transplanted sponge and the unmanipulated sponge growth rate data support prior studies showing that sponges increased growth as depth increased from shallow reefs to upper mesophotic coral reefs (Lesser 2006, Trussell et al. 2006, Lesser and Slattery 2013). Here, we show this pattern of growth extends into the mesophotic for A. tubulata on Grand Cayman reefs. The apical tag growth rates of both the transplanted and unmanipulated sponges were comparable to previous measurements of A. tubulata growth (Lesser 2006). The transplanted sponges increased growth rates in the DD and SD treatments, while the SS and DS treatments showed significantly less growth. This supports the hypothesis that the growth rate of these sponges is a response to the net effects of both biotic and abiotic factors that vary with increasing depth. In particular, no bite scars were noted on any treatment sponges suggesting that predation was not a significant factor affecting the growth of these sponges. In fact, the DS sponges actually show negative growth rates in terms of total length, potentially due to their inability to regrow tissue from the initial experimental disturbance as rapidly when compared to SD sponges. This could be the result of reductions in their food supply when they were moved to shallow depths as previously suggested (Lesser et al. 2018). Interestingly, while the deep transplanted sponges show increasing osculum width growth rates relative to their shallow counterparts, there is no change in the unmanipulated sponge osculum width growth rates as depth increases. The apparent disparity between the experimental and unmanipulated growth rates may be due to the transplanted sponges reacting to handling by thickening their osculum walls rather then putting all of the energy acquired into increasing apical growth. However, the relative osculum wall thickness growth rates in the transplant treatments were comparable to the osculum wall growth rates of naturally occurring sponges (Figs. 2B, 3B). So, naturally occurring A. tubulata are potentially prioritizing apical and linear growth over the thickening of its osculum walls as an increase in the thickness of a sponge's cell wall may limit pumping rate (Weisz et al. 2008, de Goeij et al. 2017), and therefore the ability to consume POM, while increasing size on the vertical axis provides potentially more choanocyte chambers without the inhibition of flow rate.

Increased availability and consumption of POM drives increased mesophotic growth rates

The increased consumption of POM, and PON specifically, has been proposed as a primary cause for the increased abundance, diversity, and growth rates in Caribbean mesophotic coral reef sponges (Lesser 2006, Trussell et al. 2006, Lesser and Slattery 2013, 2018, Slattery and Lesser 2015, Lesser et al. 2018, 2019, 2020). As depth increases into the mesophotic zone, picoplankton with low C:N ratios increase in abundance in this study and others (Lesser 2006, Lesser et al. 2019), which provides an important resource of organic nitrogen for active suspension feeders such as *A. tubulata* (Ribes et al. 2003, 2005). The available resources to sponges in this study show a steady

increase in POC and PON into the mesophotic zone (Fig. 4A, B), with concurrent decreases in DOC and DON (Fig. 4C, D). This pattern of trophic resource availability has been observed throughout the Caribbean Basin (Lesser 2006, Trussell et al. 2006, Lesser et al. 2019, 2020). Interestingly, this is the first time that both yearly and seasonal differences in the depth-dependent increase in POM concentration have been demonstrated for the shallow to mesophotic depth gradient in Grand Cayman, or any other location to our knowledge. Additionally, while DOM appears to be stable over time in terms of its decrease in concentration with depth, total POM availability has an inverse relationship with the availability of DIN (Appendix S1: Fig. S4) which is most likely a result of changes in water column primary productivity, and subsequent changes in the DIN pool. The DIN pool does increase with depth in both sampling periods (Appendix S1: Fig. S4), which also contributes to the greater abundances of POM along the depth gradient. In this study, the experimental sponges were producers of NO_x in January 2019, but not in July 2018 (Table 2). A similar pattern has been observed in the Xestospongia muta in the Caribbean (Southwell et al. 2008, Fiore et al. 2013), but NO_x production (i.e., whether the sponge is a source or sink) appears to vary by site (Fiore et al. 2013). Based on the results reported here, NO_x production in A. tubulata might also be affected by season (Table 2). Sponges were sources for NH₄ at both shallow and deep depths, indicating that these sponges and their microbiomes can play important roles in the cycling of these compounds at both shallow and mesophotic depths (Pita et al. 2018) (Table 2). Interestingly, while there was no significant effect of depth, sponges were generally sources for PO₄ at mesophotic depths and sinks at shallow depths. This suggests a fundamental difference in the cycling of this key nutrient by the sponge's microbiome for shallow and mesophotic sponge populations.

The availability of POM is well known to have an effect on both distributions and growth rates of a variety of active suspension feeders (Menge 2000, Gili and Coma 1998, Lesser et al. 1994, Lesser 2006, Trussell et al. 2006), and the patterns in this study reflect what has been observed for many active suspension feeders. While there are

increasing amounts of POM available to sponges in the mesophotic, the quality of that food changes along the depth gradient, and therefore could have an effect on sponge growth and abundance. It has been postulated that emergent sponges in the Caribbean are nitrogen limited on shallow reefs, and the increased nitrogen in the form of PON may allow for increased growth after respiratory demands have been met (Slattery and Lesser 2015, Lesser and Slattery 2018, Lesser et al. 2018, 2019, 2020). Many studies have identified DOC as the major contributor of carbon to sponge diets (de Goeij et al., 2013, 2017, Mueller et al. 2014, Rix et al. 2017, 2018, 2020, McMurray et al. 2018, Gantt et al. 2019, Wooster et al. 2019), such that carbon is unlikely to ever be limiting for sponges where DOC is utilized (Lesser et al. 2018, 2020). In this study, it also appears that A. tubulata is not carbon limited (Fig. 4A, C). This may, however, result in sponges becoming nitrogen limited with respect to growth (Lesser et al. 2020).

In July 2018, the SD treatment showed significantly higher consumption of POC and PON with increasing depth compared with the DS treatment, an effect reported in previous studies on sponge feeding (Lesser 2006, Trussell et al. 2006, Slattery and Lesser 2015) (Table 1). The DD treatment also showed higher consumption of POC and PON compared with the SS and DS treatments, although this was not significant. This pattern was also observed in January 2019, and while not significantly different, the DD and SD treatments showed higher consumption of POM relative to their shallow conspecifics. This increased consumption of POC, and PON in particular, would have allowed for the increased growth rates observed in this study as nitrogen is essential for growth in animals. The unmanipulated sponge feeding rates also followed this pattern of increased POM consumption mesophotic depths and significantly higher mesophotic growth rates (Table 1). Overall, this indicates that increased POM consumption is the driving force in the growth rates of these sponges.

The results of our feeding measurements confirm that *A. tubulata*, and its microbiome, also utilize significant quantities of DOM in their diets. While it has been shown that sponge cells can utilize DOM (Achlatis et al. 2019), the experimental evidence also shows that the primary

consumers of DOM within the sponge, particularly algal derived DOM, are the prokaryotic microbiome (Zhang et al. 2019, Rix et al. 2020) which can then transform and translocate DOM to the host (Shih et al. 2020). The microbiome of A. tubulata, particularly the high proportion of Chloroflexi bacteria, has also been shown to have broad metabolic potential for the use of labile, semi-labile, and refractory DOM. However, it is unknown what proportion of this DOM is provided to A. tubulata from its microbiome in the form of translocated products or via the phagocytosis of symbionts (Leys et al. 2018, Shih et al. 2020). The proportional uptake of POC to DOC (2–4% and 96–98%, respectively) found in this experiment was similar to values on emergent HMA sponges on coral reefs (de Goeij et al. 2017, Wooster et al. 2019), but the POC proportion was lower than observed in other studies (McMurray et al. 2018, Rix et al. 2020). While DOM is potentially important for the microbiome of sponges, it is clear that POM is crucial for the sponge host, as a large component of nitrogen is derived from feeding on POM in sponges (Lesser et al. 2020, Bart et al. 2020).

Stable isotopes of transplanted sponges reflect increased reliance on POM in the mesophotic

The increased use of POM as a nutritional resource for sponge communities in the mesophotic zone of the Caribbean is reflected in the stable isotopic signatures of A. tubulata tissue. Stable isotopes are generally considered a time integrated metric for assessing the diet of an organism (Fry 2006), and while there are no published studies on stable isotope turnover in sponges, we can estimate their half-life in sponges using the equation for whole body invertebrate samples provided by Vander Zanden et al. (2015). Sponges in this study had an average mass of 29.15 g AFDW with an estimated stable isotope half-life of -56 d. The small increase in δ^{13} C may be the result of reduced consumption of photoautotrophically derived DOM and POM. It is unlikely due to depthdependent changes in symbiont function, as A. tubulata has no known photoautotrophic symbionts (Gantt et al. 2019, Macartney KJ & Lesser MP, unpublished) where the fractionation of carbon would have been affected by decreasing E_d with depth. The increased $\delta^{15}N$ at the deep site mirrors similar patterns observed in other sponges along a shallow to mesophotic depth gradient (Slattery et al. 2011, Morrow et al. 2016). The stable δ^{15} N isotope is often used as a measure of heterotrophy and changes in trophic position (Peterson and Fry 1987). In A. tubulata, POM concumption increases with increasing depth (Slattery et al. 2011), and the increased δ¹⁵N suggests an increased reliance by mesophotic sponges on resources such as heterotrophic picoplankton or prochlorophytes, both of which increase in the mesophotic in this study and others (e.g., Lesser et al. 2019, 2020), compared to isotopically lighter eukaryotic phytoplankton and autotrophic picoplankton such as Synechococcus (Lesser 2006, Lesser et al. 2019, 2020; this study). The decrease in C:N ratios at the deep site also indicates that deep sponges have a more stoichiometrically balanced diet to start with, relative to shallow sponges (Lesser et al. 2020). Taken together, the stable isotope data, feeding measurements, and ambient POM concentrations provide compelling evidence that the observed differences in growth were driven by the consumption of nitrogen-rich POM over time, on mesophotic reefs relative to shallow reefs. This increased consumption of an abundant, nitrogen-rich resource with greater bioavailability at mesophotic depths supports higher growth rates on MCEs. This is the most parsimonious explanation based on the data presented here, previously published literature on Caribbean sponges (Lesser 2006, Trussell et al. 2006, Lesser and Slattery 2013, Slattery and Lesser 2015, Wulff 2017) and literature on other active suspension feeders from a variety of environments (Lesser et al. 1994, Menge et al. 1994, Gili and Coma 1998, Menge 2000, Gili et al. 2001, Lesser and Slattery 2015).

In some cases, other factors have been shown to regulate the distribution and abundance of active suspension feeders (i.e., predation or physical disturbances: Menge and Sutherland 1976, Summerson and Peterson 1984, Wulff 2017), but the results of this study show that bottom-up forces (i.e., food availability) are an important factor regulating sponge biomass and growth rates. Top-down control, in the form of predation, also seems unlikely here as *A. tubulata* is a chemically defended sponge that produces a wide variety of secondary metabolites, resulting

in tissue extracts from this sponge becoming less palatable to spongivores relative to other sponge species (Chanas et al. 1997, Assmann et al. 2000, Pawlik 2011). Also, in this experiment no bite scars from spongivorous fish were observed on naturally occurring or transplanted sponges. Since these sponges were exposed to all abiotic and biotic factors, the lack of bite scars suggests that predation was not a confounding factor affecting the growth rates observed during this experiment. There also does not appear to be any effects of the sponge racks on experimental sponges (Appendix S1: Fig. S1) as there were no signs of damage on the outer wall of the sponges. This is further supported by the observations of Wulff (2017) who found that predation was not a significant regulator of sponge populations between depths on coral reefs but did structure sponge populations between different habitats (e.g., mangrove vs. coral reef). The potential for phenotypic plasticity in chemical defense strategy and tissue regeneration along a depth gradient has been shown before in the sponge P. angulospiculatus, where shallow conspecifics prioritized chemical defense over tissue regeneration (Slattery et al. 2016). This trade-off does not appear to have occurred here, as we noted increased apical growth in experimental mesophotic sponges indicating that these sponges were prioritizing overall growth, not just tissue regeneration, rather than defense against potential predators (sensu Ferretti et al. 2009).

It is also unlikely the light environment had any direct effect on this sponge's growth rates or metabolic requirements due to the lack of photoautotrophic symbionts in *A. tubulata* (Gantt et al. 2019; Macartney KJ & Lesser MP, *unpublished*). *A. tubulata* does harbor dense *Chloroflexi* populations (Gantt et al. 2019), as observed in many Caribbean sponges (Hentschel et al. 2012, Thomas et al. 2016, Pita et al. 2018), and while these bacteria have the potential for phototrophic metabolism (3-hydroxypropionate pathway: Ward et al. 2018), this was not reflected in the sponge tissue isotopic composition (Canfield et al. 2005).

CONCLUSIONS

The results of this study show that *A. tubulata* in the mesophotic have greater growth rates

relative to their shallow conspecifics. Particulate organic matter was also significantly higher at mesophotic depths in both July and January, which provides evidence that the increased growth rates at mesophotic depths were a result of the increased consumption of abundant POM available to the mesophotic sponges. This was confirmed by the sponge tissue δ^{15} N values and feeding measurements. We have also shown that A. tubulata consumes significant concentrations of DOC and DON. But given the higher C:N ratios and lower bioavailability of DOM for sponges, the amount of this DOM that actually goes into sponge biomass accumulation (sensu Shih et al. 2020) is unknown. These sponges were found to be sources of inorganic and organic compounds such as NO_x, NH₄, and SiO₂ at our site and were sources for PO₄ at mesophotic depths, illustrating the important role A. tubulata may also play in the local cycling of these essential nutrients for many community members on shallow and mesophotic coral reefs (sensu Slattery et al. 2013). Further studies on the cycling of inorganic and organic compounds by sponges on MCEs, their chemical composition, and microbial community structure along the shallow to mesophotic depth gradient are necessary. These data will help identify other factors controlling the growth, biomass, and distribution of this Caribbean coral reef sponge.

ACKNOWLEDGMENTS

We thank E. Kintzing, D. Gochfeld, and A. Chaves Chaves Fonnegra for field and laboratory support. We thank A. Weinheimer for insightful comments on the manuscript draft and statistical analyses. We thank S. Pankey for field and laboratory support and assistance with statistical analyses. All sample collections complied with the laws of the Cayman Islands and the United States of America. Logistical support was provided to the staff of InDepth Water Sports in Grand Cayman. Support was provided by NSF Biological Oceanography (OCE–1632348/1632333) to MPL and MS, respectively, and the University of New Hampshire Marine Biology Small Grants fund to KJM.

LITERATURE CITED

Achlatis, M., M. Pernice, K. Green, J. M. de Goeij, P. Guagliardo, M. R. Kilburn, O. Hoegh-Guldberg, and S. Dove. 2019. Single-cell visualization

- indicates direct role of sponge host in uptake of dissolved organic matter. Proceedings of the Royal Society B: Biological Sciences 286(1916):20192153. http://dx.doi.org/10.1098/rspb.2019.2153
- Assmann, M., E. Lichte, J. R. Pawlik, and M. Köck. 2000. Chemical defenses of the Caribbean sponges *Agelas wiedenmayeri* and *Agelas conifera*. Marine Ecology Progress Series 207:255–262.
- Bart, M. C., A. de Kluijver, S. Hoetjes, S. Absalah, B. Mueller, E. Kenchington, H. T. Rapp, and J. M. de Goeij. 2020. Differential processing of dissolved and particulate organic matter by deep-sea sponges and their microbial symbionts. Scientific Reports 10(1). http://dx.doi.org/10.1038/s41598-020-74670-0
- Bell, J. J. 2008. The functional roles of marine sponges. Estuarine, Coastal and Shelf Science 79: 341–353.
- Bertilsson, S., O. Berglund, D. M. Karl, and S. W. Chisholm. 2003. Elemental composition of marine Prochlorococcus and Synechococcus: implications for the ecological stoichiometry of the sea. Limnology and Oceanography 48:1721–1731.
- Boudreaux, M. L., J. L. Stiner, and L. J. Walters. 2006. Biodiversity of sessile and motile macrofauna on intertidal oyster reefs in Mosquito Lagoon, Florida. Journal of Shellfish Research 25:1079–1089.
- Bradford, M. M. 1976. A rapid and sensitive method for the quantitation of microgram quantities of protein utilizing the principle of protein-dye binding. Analytical biochemistry 72:248–254.
- Campbell, L., H. A. Nolla, and D. Vaulot. 1994. The importance of Prochlorococcus to community structure in the central North Pacific Ocean. Limnology and Oceanography 39:954–961.
- Canfield, D. E., E. Kristensen, and B. Thamdrup. 2005. Carbon fixation and phototrophy. Pages 95–127 *in* Advances in marine biology. Volume 48. Cambridge: Academic Press.
- Cattaneo-Vietti, R., M. Chiantore, C. Misic, P. Povero, and M. Fabiano. 1999. The role of pelagic-benthic coupling in structuring littoral benthic communities at Terra Nova Bay (Ross Sea) and in the Straits of Magellan. Scientia Marina 63:113–121.
- Chanas, B., J. R. Pawlik, T. Lindel, and W. Fenical. 1997. Chemical defense of the Caribbean sponge Agelas clathrodes (Schmidt). Journal of Experimental Marine Biology and Ecology 208(1–2):185–196.
- Coppari, M., A. Gori, N. Viladrich, L. Saponari, A. Canepa, J. Grinyó, A. Olariaga, and S. Rossi. 2016. The role of Mediterranean sponges in benthic-pelagic coupling processes: *Aplysina aerophoba* and *Axinella polypoides* case studies. Journal of Experimental Marine Biology and Ecology 477: 57–68.

- Dayton, P. K., G. A. Robilliard, R. T. Paine, and L. B. Dayton. 1974. Biological accommodation in the benthic community at McMurdo Sound, Antarctica. Ecological Monographs 44:105–128.
- de Goeij, J. M., M. P. Lesser, and J. R. Pawlik. 2017. Nutrient fluxes and ecological functions of coral reef sponges in a changing ocean. Pages 373–410 *in* Climate change, ocean acidification and sponges. New York: Springer.
- de Goeij, J. M., L. Moodley, M. Houtekamer, N. M. Carballeira, and F. C. Van Duyl. 2008. Tracing 13C-enriched dissolved and particulate organic carbon in the bacteria-containing coral reef sponge *Halisarca caerulea*: evidence for DOM-feeding. Limnology and Oceanography 53:1376–1386.
- de Goeij, J. M., D. Van Oevelen, M. J. Vermeij, R. Osinga, J. J. Middelburg, A. F. De Goeij, and W. Admiraal. 2013. Surviving in a marine desert: The sponge loop retains resources within coral reefs. Science 342:108–110.
- Diaz, M. C., and K. Rützler. 2001. Sponges: an essential component of Caribbean coral reefs. Bulletin of Marine Science 69:535–546.
- Ducklow, H. W., D. L. Kirchman, H. L. Quinby, C. A. Carlson, and H. G. Dam. 1993. Stocks and dynamics of bacterioplankton carbon during the spring bloom in the eastern North Atlantic Ocean. Deep Sea Research Part II: Topical Studies in Oceanography 40:245–263.
- Fagerbakke, K. M., M. Heldal, and S. Norland. 1996. Content of carbon, nitrogen, oxygen, sulfur and phosphorus in native aquatic and cultured bacteria. Aquatic Microbial Ecology 10:15–27.
- Ferretti, C., S. Vacca, C. De Ciucis, B. Marengo, A. R. Duckworth, R. Manconi, R. Pronzato, and C. Domenicotti. 2009. Growth dynamics and bioactivity variation of the Mediterranean demosponges Agelas oroides (Agelasida, Agelasidae) and Petrosia ficiformis (Haplosclerida, Petrosiidae). Marine Ecology 30:327–336.
- Fiore, C. L., D. M. Baker, and M. P. Lesser. 2013. Nitrogen biogeochemistry in the Caribbean sponge, *Xestospongia muta*: A source or sink of dissolved inorganic nitrogen? PLOS ONE 8:e72961.
- Fiore, C. L., J. K. Jarett, G. Steinert, and M. P. Lesser. 2020. Trait-based comparison of coral and Sponge Microbiomes. Scientific reports 10:1–16.
- Freeman, C. J., and R. W. Thacker. 2011. Complex interactions between marine sponges and their symbiotic microbial communities. Limnology and Oceanography 56:1577–1586.
- Freeman, N. K., F. T. Lindgren, Y. O. Ng, and A. V. Nichols. 1952. Infrared spectra of some lipoproteins and related lipids. Journal of Biological Chemistry 203:293–304.

- Fry, B. 2006. Stable Isotope Ecology. Volume 521. New York: Springer.
- Gantt, S. E., S. E. McMurray, A. D. Stubler, C. M. Finelli, J. R. Pawlik, and P. M. Erwin. 2019. Testing the relationship between microbiome composition and flux of carbon and nutrients in Caribbean coral reef sponges. Microbiome 7:124.
- Gili, J. M., and R. Coma. 1998. Benthic suspension feeders: their paramount role in littoral marine food webs. Trends in ecology & evolution 13:316–321.
- Gili, J. M., R. Coma, C. Orejas, P. J. López-González, and M. Zabala. 2001. Are Antarctic suspensionfeeding communities different from those elsewhere in the world? Polar Biology 24:473–485.
- Hentschel, U., J. Piel, S. M. Degnan, and M. W. Taylor. 2012. Genomic insights into the marine sponge microbiome. Nature Reviews Microbiology 10:641– 654.
- Jaschinski, S., T. Hansen, and U. Sommer. 2008. Effects of acidification in multiple stable isotope analyses. Limnology and Oceanography: Methods 6:12–15.
- Kolasinski, J., K. Rogers, and P. Frouin. 2008. Effects of acidification on carbon and nitrogen stable isotopes of benthic macrofauna from a tropical coral reef. Rapid Communications in Mass Spectrometry 22:2955–2960.
- Lawrence, J. M. 1973. Level, content, and caloric equivalents of the lipid, carbohydrate, and protein in the body components of Luidia clathrata (echinodermata: asteroidea: platyasterida) in Tampa bay. Journal of Experimental Marine Biology and Ecology 11(3):263–274.
- Lesser, M. P. 2006. Benthic–pelagic coupling on coral reefs: feeding and growth of Caribbean sponges. Journal of Experimental Marine Biology and Ecology 328:277–288.
- Lesser, M. P., and V. A. Kruse. 2004. Seasonal temperature compensation in the horse mussel, *Modiolus modiolus*: metabolic enzymes, oxidative stress and heat shock proteins. Comparative Biochemistry and Physiology Part A: Molecular & Integrative Physiology 137(3):495–504.
- Lesser M. P., B. Mueller, M. S. Pankey, K. J. Macartney, M. Slattery, J. M. de Goeij. 2020. Depth-dependent detritus production in the sponge, Halisarca caerulea. Limnology and Oceanography 65(6):1200–1216.
- Lesser, M. P., and M. Slattery. 2013. Ecology of Caribbean sponges: Are top-down or bottom-up processes more important? PLOS ONE 8:e79799.
- Lesser, M. P., and M. Slattery. 2015. Picoplankton consumption supports the ascidian *Cnemidocarpa verrucosa* in McMurdo Sound, Antarctica. Marine Ecology Progress Series 525:117–126.

- Lesser, M. P., and M. Slattery. 2018. Sponge density increases with depth throughout the Caribbean. Ecosphere 9:e02525.
- Lesser, M. P., M. Slattery, J. H. Laverick, K. J. Macartney, and T. C. Bridge. 2019. Global community breaks at 61 m on mesophotic coral reefs. Global Ecology and Biogeography 28:1403–1416.
- Lesser, M. P., M. Slattery, and J. J. Leichter. 2009. Ecology of mesophotic coral reefs. Journal of Experimental Marine Biology and Ecology 375:1–8.
- Lesser, M. P., M. Slattery, and C. D. Mobley. 2018. Biodiversity and functional ecology of mesophotic coral reefs. Annual Review of Ecology, Evolution, and Systematics 49:49–71.
- Lesser, M. P., J. D. Witman, and K. P. Sebnens. 1994. Effects of flow and seston availability on scope for growth of benthic suspension-feeding invertebrates from the Gulf of Maine. The Biological Bulletin 187:319–335.
- Leys, S. P., A. S. Kahn, J. K. H. Fang, T. Kutti, and R. J. Bannister. 2018. Phagocytosis of microbial symbionts balances the carbon and nitrogen budget for the deep-water boreal sponge *Geodia barretti*. Limnology and Oceanography 63:187–202.
- Lomas, M. W., D. K. Steinberg, T. Dickey, C. A. Carlson, N. B. Nelson, R. H. Condon, and N. R. Bates. 2010. Increased ocean carbon export in the Sargasso Sea linked to climate variability is countered by its enhanced mesopelagic attenuation. Biogeosciences 7(1):57–70.
- Loya, Y., G. Eyal, T. Treibitz, M. P. Lesser, and R. Appeldoorn. 2016. Theme section on mesophotic coral ecosystems: advances in knowledge and future perspectives. Coral Reefs 35:1–9.
- Macartney, K. J., M. Slattery, and M. P. Lesser. 2021. Trophic ecology of Caribbean sponges in the mesophotic zone. Limnology and Oceanography 66:1113–1124.
- Maldonado, M., M. Ribes, and F. C. van Duyl. 2012. Nutrient fluxes through sponges: biology, budgets, and ecological implications. Pages 113–182 *in* Advances in marine biology. Volume 62. Cambridge: Academic Press.
- Marie, D., N. Simon, and D. Vaulot. 2005. Phytoplankton cell counting by flow cytometry. Algal Culturing Techniques 1:253–267.
- Masuko, T., A. Minami, N. Iwasaki, T. Majima, S. I. Nishimura, and Y. C. Lee. 2005. Carbohydrate analysis by a phenol–sulfuric acid method in microplate format. Analytical Biochemistry 339:69–72.
- McClintock, J. B., J. Heine, M. Slattery, and J. Weston. 1991. Biochemical and energetic composition, population biology, and chemical defense of the antarctic ascidian Cnemidocarpa verrucosa lesson.

- Journal of Experimental Marine Biology and Ecology 147(2):163–175.
- McMurray, S. E., A. D. Stubler, P. M. Erwin, C. M. Finelli, and J. R. Pawlik. 2018. A test of the spongeloop hypothesis for emergent Caribbean reef sponges. Marine Ecology Progress Series 588:1–14.
- Menge, B. A. 2000. Top-down and bottom-up community regulation in marine rocky intertidal habitats. Journal of Experimental Marine Biology and Ecology 250(1–2):257–289.
- Menge, B. A., and J. P. Sutherland. 1976. Species Diversity Gradients: Synthesis of the Roles of Predation, Competition, and Temporal Heterogeneity. The American Naturalist 110(973):351–369.
- Menge, B. A., E. L. Berlow, C. A. Blanchette, S. A. Navarrete, and S. B. Yamada. 1994. The keystone species concept: variation in interaction strength in a rocky intertidal habitat. Ecological Monographs 64:249–286.
- Morel, A., Y. H. Ahn, F. Partensky, D. Vaulot, and H. Claustre. 1993. Prochlorococcus and Synechococcus: a comparative study of their optical properties in relation to their size and pigmentation. Journal of Marine Research 51:617–649.
- Morrow, K. M., C. L. Fiore, and M. P. Lesser. 2016. Environmental drivers of microbial community shifts in the giant barrel sponge, *Xestospongia muta*, over a shallow to mesophotic depth gradient. Environmental Microbiology 18:2025–2038.
- Mueller, B., J. M. de Goeij, M. J. Vermeij, Y. Mulders, E. van der Ent, M. Ribes, and F. C. van Duyl. 2014. Natural diet of coral-excavating sponges consists mainly of dissolved organic carbon (DOC). PLOS ONE 9:e90152.
- Packard, G. C., and T. J. Boardman. 1988. The misuse of ratios, indices, and percentages in ecophysiological research. Physiological Zoology 61:1–9.
- Pawlik, J. R. 2011. The chemical ecology of sponges on Caribbean reefs: Natural products shape natural systems. BioScience 61:888–898.
- Pawlik, J. R., B. Chanas, R. J. Toonen, W. Fenical. 1995. Defenses of Caribbean sponges against predatory reef fish. I. Chemical deterrency. Marine Ecology Progress Series 127:183–194.
- Perea-Blazquez, A., S. K. Davy, and J. J. Bell. 2012. Estimates of particulate organic carbon flowing from the pelagic environment to the benthos through sponge assemblages. PLOS ONE 7:e29569.
- Peterson, B. J., and B. Fry. 1987. Stable Isotopes in Ecosystem Studies. Annual Review of Ecology and Systematics 18(1):293–320.
- Pile, A. J., M. R. Patterson, M. Savarese, V. I. Chernykh, and V. A. Fialkov. 1997. Trophic effects of sponge feeding within Lake Baikal's littoral zone. 2. Sponge abundance, diet, feeding efficiency, and

- carbon flux. Limnology and Oceanography 42: 178–184
- Pita, L., L. Rix, B. M. Slaby, A. Franke, and U. Hentschel. 2018. The sponge holobiont in a changing ocean: from microbes to ecosystems. Microbiome 6:46.
- Ribes, M., R. Coma, M. J. Atkinson, and R. A. Kinzie III. 2003. Particle removal by coral reef communities: Picoplankton is a major source of nitrogen. Marine Ecology Progress Series 257:13–23.
- Ribes, M., R. Coma, M. J. Atkinson, and R. A. Kinzie III. 2005. Sponges and ascidians control removal of particulate organic nitrogen from coral reef water. Limnology and Oceanography 50:1480–1489.
- Richelle-Maurer, E., M. J. De Kluijver, S. Feio, S. Gaudêncio, H. Gaspar, R. Gomez, R. Tavares, G. Van de Vyver, and R. W. M Van Soest. 2003. Localization and ecological significance of oroidin and sceptrin in the Caribbean sponge Agelas conifera. Biochemical Systematics and Ecology 31(10):1073–1091.
- Rix, L., J. M. de Goeij, D. van Oevelen, U. Struck, F. A. Al-Horani, C. Wild, and M. S. Naumann. 2017. Differential recycling of coral and algal dissolved organic matter via the sponge loop. Functional Ecology 31:778–789.
- Rix, L., J. M. de Goeij, D. van Oevelen, U. Struck, F. A. Al-Horani, C. Wild, and M. S. Naumann. 2018. Reef sponges facilitate the transfer of coral-derived organic matter to their associated fauna via the sponge loop. Marine Ecology Progress Series 589:85–96.
- Rix, L., M. Ribes, R. Coma, M. T. Jahn, J. M. de Goeij, D. van Oevelen, S. Escrig, A. Meibom, and U. Hentschel. 2020. Heterotrophy in the earliest gut: a single-cell view of heterotrophic carbon and nitrogen assimilation in sponge-microbe symbioses. ISME Journal 14:2554–2567.
- Saier, B. 2002. Subtidal and intertidal mussel beds (Mytilus edulis L.) in the Wadden Sea: diversity differences of associated epifauna. Helgoland Marine Research 56:44–50.
- Sieracki, M. E., P. G. Verity, and D. K. Stoecker. 1993. Plankton community response to sequential silicate and nitrate depletion during the 1989 North Atlantic spring bloom. Deep Sea Research Part II: Topical Studies in Oceanography 40(1–2):213–225.
- Shih, J. L., K. E. Selph, C. B. Wall, N. J. Wallsgrove, M. P. Lesser, and B. N. Popp. 2020. Trophic ecology of the tropical pacific sponge *Mycale grandis* inferred from amino acid compound-specific isotopic analyses. Microbial Ecology 79:495–510.
- Slattery, M., D. J. Gochfeld, M. C. Diaz, R. W. Thacker, and M. P. Lesser. 2016. Variability in chemical

- defense across a shallow to mesophotic depth gradient in the Caribbean sponge *Plakortis angulospiculatus*. Coral Reefs 35:11–22.
- Slattery, M., D. J. Gochfeld, C. G. Easson, and L. R. O'Donahue. 2013. Facilitation of coral reef biodiversity and health by cave sponge communities. Marine Ecology Progress Series 476:71–86.
- Slattery, M. 2015. Trophic ecology of sponges from shallow to mesophotic depths (3 to 150 m): comment on Pawlik et al. (2015). Marine Ecology Progress Series 527: 275–279.
- Slattery, M., and M. P. Lesser. 2019. The Bahamas and Cayman Islands. Pages 47–56 *in* Mesophotic coral ecosystems. Springer, Cham, Switzerland.
- Slattery, M., M. P. Lesser, D. Brazeau, M. D. Stokes, and J. J. Leichter. 2011. Connectivity and stability of mesophotic coral reefs. Journal of Experimental Marine Biology and Ecology 408:32–41.
- Southwell, M. W., J. B. Weisz, C. S. Martens, and N. Lindquist. 2008. In situ fluxes of dissolved inorganic nitrogen from the sponge community on Conch Reef, Key Largo, Florida. Limnology and Oceanography 53(3):986–996.
- Summerson, H. C., and C. H. Peterson. 1984. Role of predation in organizing benthic communities of a temperate-zone seagrass bed. Marine Ecology Progress Series 15(1):63–77.
- Thacker, R. W., and C. J. Freeman. 2012. Spongemicrobe symbioses. Recent Advances and New Directions, Advances in Marine Biology 62:57–111.
- Thomas, T., L. Moitinho-Silva, M. Lurgi, J. R. Björk, C. Easson, C. Astudillo-García, and A. Chaves-Fonnegra. 2016. Diversity, structure and convergent evolution of the global sponge microbiome. Nature Communications 7:1–12.
- Trussell, G. C., M. P. Lesser, M. R. Patterson, and S. J. Genovese. 2006. Depth-specific differences in growth of the reef sponge *Callyspongia vaginalis*: role of bottom-up effects. Marine Ecology Progress Series 323:149–158.
- Vafeiadou, A. M., H. Adão, M. De Troch, and T. Moens. 2013. Sample acidification effects on carbon and nitrogen stable isotope ratios of macrofauna from a *Zostera noltii* bed. Marine and Freshwater Research 64:741–745.
- Vander Zanden, M. J., M. K. Clayton, E. K. Moody, C. T. Solomon, and B. C. Weidel. 2015. Stable isotope turnover and half-life in animal tissues: a literature synthesis. PLOS ONE 10:e0116182.
- Verity, P. G., C. Y. Robertson, C. R. Tronzo, M. G. Andrews, J. R. Nelson, and M. E. Sieracki. 1992. Relationships between cell volume and the carbon and nitrogen content of marine photosynthetic nanoplankton. Limnology and Oceanography 37:1434–1446.

- Ward, L. M., J. Hemp, P. M. Shih, S. E. McGlynn, and W. W. Fischer. 2018. Evolution of phototrophy in the Chloroflexi phylum driven by horizontal gene transfer. Frontiers in Microbiology 9:260.
- Weisz, J. B., N. Lindquist, and C. S. Martens. 2008. Do associated microbial abundances impact marine demosponge pumping rates and tissue densities? Oecologia 155:367–376.
- Wooster, M. K., S. E. McMurray, J. R. Pawlik, X. A. Morán, and M. L. Berumen. 2019. Feeding and
- respiration by giant barrel sponges across a gradient of food abundance in the Red Sea. Limnology and Oceanography 64:1790–1801.
- Wulff, J. 2017. Bottom-up and top-down controls on coral reef sponges: disentangling within-habitat and between-habitat processes. Ecology 98:1130–1139.
- Zhang, F., L. Jonas, H. Lin, and R. T. Hill. 2019. Microbially mediated nutrient cycles in marine sponges. FEMS Microbiology Ecology 95:115.

SUPPORTING INFORMATION

 $Additional\ Supporting\ Information\ may\ be\ found\ online\ at:\ http://onlinelibrary.wiley.com/doi/10.1002/ecs2.$ 3764/full